# MEASUREMENT OF THE LATERAL NOISE EMISSION OF AN UIC 60 RAIL WITH A CUSTOM DEVICE

A. Bracciali and G. Cascini

*Dipartimento di Meccanica e Tecnologie Industriali, Università degli Studi di Firenze, via Santa Marta 3, 50139 Firenze, Italy*

In this work a simplified device for the measurement of the noise emitted laterally by an UIC 60 rail is presented. It consists of three convergent parallel ducts with an anechoic termination to collect the sound energy in a straight, cross-square section pipe where measuring microphones are located. The acoustic design of the device is described with reference to the shape definition, based on FEM analysis, and to the optimization of the multilayered anechoic termination with experimental and numerical techniques. Laboratory tests performed to calibrate and to validate the device are shown and its acoustical performance is analyzed and discussed. The overall dimension and the very limited weight of the device ensures the portability and hence its practical use; the limited cost and the use with standard instrumentation make possible its use for the detection of an excessive wear of wheel tread. The results of the first application of the device are shown, and a comparison is made between the noise emitted by the rail head, the rail web and the rail foot at the passage of damaged and non-damaged wheels.

© 2000 Academic Press

## 1. INTRODUCTION

The different contribution of rail and wheel to global railway noise is fundamental in all railway noise generation and propagation analyses. Several authors dealt with the question and comprehensive reference lists can be found in the proceedings of past IWRN workshops. The main engineering problem is the intrinsic difficulty in measuring the two sources separately: the contact zone is very limited in space, and the speed of the train is anyway too high to result in anything other than a very limited duration of local emission. The problem has been approached by examining acoustical measurement techniques which are capable of "following" the moving train; the development of methods using an array of microphones is also important. All of these methods are based on advanced techniques using several microphones that perform a sweep which is capable of eliminating the frequency shift (Doppler effect) due to the train speed. The results are significant from an engineering point of view, because they allow the location of sources on a line or on a plane. However, these systems are inevitably quite complicated both in terms of instrumentation and software post-processing.

The authors developed in the past few years a device to measure noise under the axlebox of any rolling stock [1–3]. This device is insensitive to air flow and allowed fast and reliable measurements up to 300 km/h. Obviously, the axlebox area contains much machinery (primary suspension springs, axlebox body and guiding links, dampers) and this necessitates locating the device just under the axlebox, where the measured noise is a combination of rail and wheel noise.

In this paper a new device to measure the noise emitted only by the rail is proposed. It is made of three parallel converging ducts which allows the noise emitted by the head, the web and the foot of an UIC 60 rail to be measured separately. Several constraints, both acoustical and mechanical, that had to be faced to obtain a reliable device are briefly described; some results of the first application of the device are then presented and discussed.

## 2. ACOUSTICAL DESIGN OF A NOISE COLLECTOR

The collection of noise emitted by a vibrating surface contrasts with the requirement to know the exact magnitude and phase relationship of the sound emitted by the several portions of the surface. Any collector will, in fact, combine these components such that the measured sound pressure level will only be meaningful from the energy point of view. In spite of this, such a device proves nonetheless to be extremely useful in such situations where the application of more conventional techniques is not possible. Both the array of microphones and the sound intensity techniques can be usefully complemented by the noise collector, primarily for cost reasons in the former case, and in both cases for the application in highly reactive fields where the isolation of the real component of sound intensity proves to be difficult.

The noise collector partially overcomes another typical problem in the measurement of non-stationary noises, namely the duration of the noise emission. For purely random noise sources, and with good approximation also for wide band noise sources, the relationship that links the bandwidth $B$ of the analogue or digital filter and the integration time $T$ is such that $BT > 1$ must hold. When transient phenomena are very fast, sweeping techniques are obviously the best, but the artificial increase of the measurement duration by collecting the noise from a larger portion of the surface of the emitter can also help.

### 2.1. DEFINITION OF THE SHAPE

The propagation of a plane wave along a cylindrical duct with a continuously variable cross-section (horn) is governed by the mass and energy conservation equations and by the choice of the thermodynamic transformation that the fluid undergoes (typically an isentropic one). The differential equation that results can be solved only for some particularly simple duct shapes like a conical or exponential horn [4]. For the latter, the cross-section $S$ is a function of the abscissa $z$ of the horn and of the inlet cross-section $S_0$ by the law $S = S_0 e^{mz}$ and the impedance seen from

the inlet section is given by

$$Z = \frac{\rho c}{S_0}\left(\sqrt{1 - \frac{m^2}{4k^2}} + j\frac{m}{2k}\right), \tag{1}$$

where $k = \omega/c$ is the wavenumber, $c$ is the sound speed in the air, and $f_c = mc/4\pi$ defines the so-called *cut-off frequency*, below which no sound power is transmitted along the horn. In this case the impedance is purely reactive and a loudspeaker in the inlet section would not be able to radiate sound power at the outlet section.

The authors did not find in the literature general analytical solutions for collecting (and not radiating) horns where the incoming wave is not plane but generic. Moreover, the use of non-circular cross-section horns is even more unusual, as the cylindrical symmetry allows the sound power emitted (that is the normal situation for loudspeakers!) to be maximized above the cut-off frequency and reduces the analytical problem to a mono-dimensional one. The noise collector developed in this research has a rectangular cross-section with constant height: to evaluate to a first degree of approximation whether the chosen dimensions ($30 \times 5$ cm at the inlet, $5 \times 5$ cm at the outlet, length of the horn $= 35$ cm) can be a good basis for the development, the impedance seen by a plane wave entering the duct with an equivalent circular cross-sections was calculated, showing a dramatic increase below 100 Hz. The $5 \times 5$ cm outlet section is such that plane waves can develop, at an appropriate distance from the converging duct, up to 3400 Hz without the rise of lateral acoustical eigenmodes. Clearly, this approximation is too rough to be retained without further investigation, and extensive simulations have been made by using a FEM code with acoustic capabilities [5]. Three shapes of the rectangular duct were tested, namely linear, cubic and exponential. The shapes and a sketch of the linear horn are shown in Figure 1 where, at the end of the straight duct, the anechoic termination described below must be added (it has been taken into account in the FEM simulation by adopting an absorption coefficient of $\alpha = 0.9$).
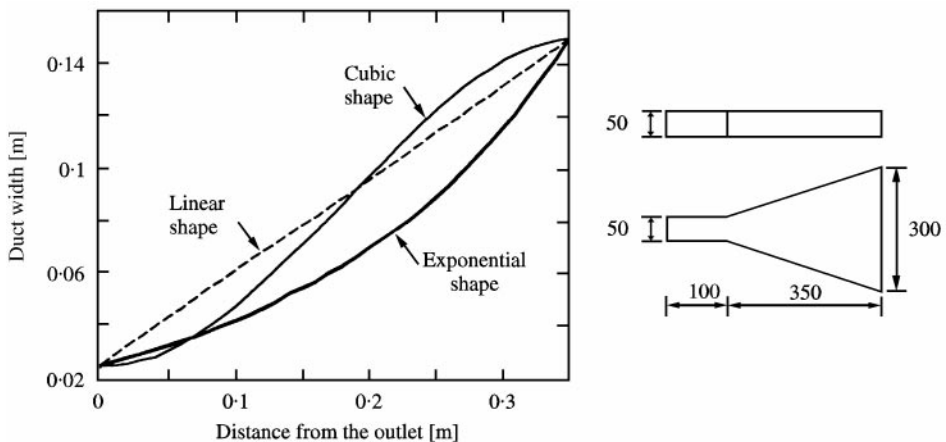


Figure 1. Lateral shapes used in numerical simulations (left) and overall dimensions for linear-shaped duct (right).
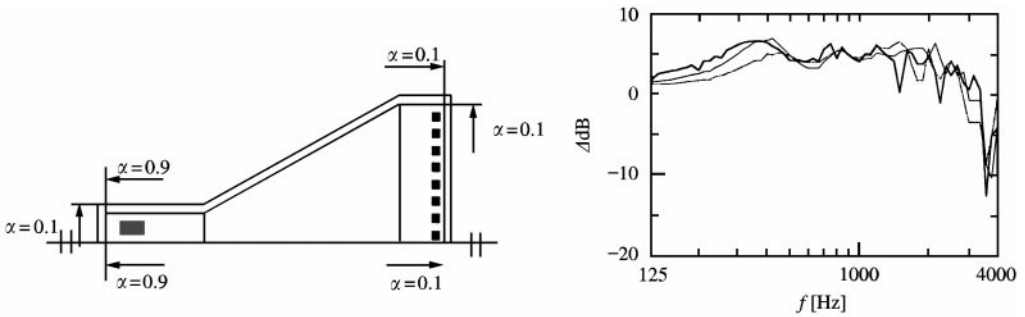
Figure 2. 2-D FEM model with boundary conditions for linear shape duct (left); SPL calculated in the averaging area normalised w.r.t. the average inlet SPL for the three duct shapes (right). ■, monopolar sources; ▬, area where average SPL is evaluated. Lateral shape of the converging duct: —, linear; ——, exponential; ———, cubic.

The simulation has been performed in 2-D and in 3-D with the boundary conditions shown in Figure 2. Noise sources are monopoles with random amplitude in the range $113 \pm 2$ dB (ref. 20 μPa) and random phase, placed at 30 mm from the inlet section. Acoustic finite elements sizes are such that there are at least 20 elements per wavelength at the higher frequencies, a condition that proved to be fundamental to obtain sufficiently stable results [6].

The fast 2-D simulations showed that the $\frac{1}{12}$ octave bands in the range 125 Hz–4 kHz are almost insensitive to the shape, and that there is no reason to complicate the practical construction of the horn. This can be easily justified recalling that the inlet wavefront is not plane, the cross-section is not cylindrical and that the duct is converging and not diverging. The behaviour shown in Figure 2 is very flat up to 3·4 kHz where lateral resonances take up importance.

Three-dimensional simulations are more complex and did not lead to different results, such that the bi-dimensionality hypothesis can be retained with a very good degree of approximation. An example of the comparison of 2-D and 3-D results is shown in Figure 3.

2.2. OPTIMIZATION OF THE ANECHOIC TERMINATION

The necessity of an anechoic termination can be easily understood considering that only this condition, together with the plane wave condition already referred to, allows the measurement of the noise in the straight pipe by means of a single microphone flush-mounted. The only way to absorb a plane wave broadband noise efficiently is to stack a number of layers of sound absorbing porous materials [7]. The determination of the length and of the acoustic properties of the layers is not trivial, apart from the physical and intuitive consideration that flow resistance should increase and layer length should decrease in the direction of the travelling wave. The optimization process obviously required some constraints: the overall length of the termination (which must be portable), the maximum number of layers (limited to 3 or 4 materials), the minimum thickness of each layer (very low
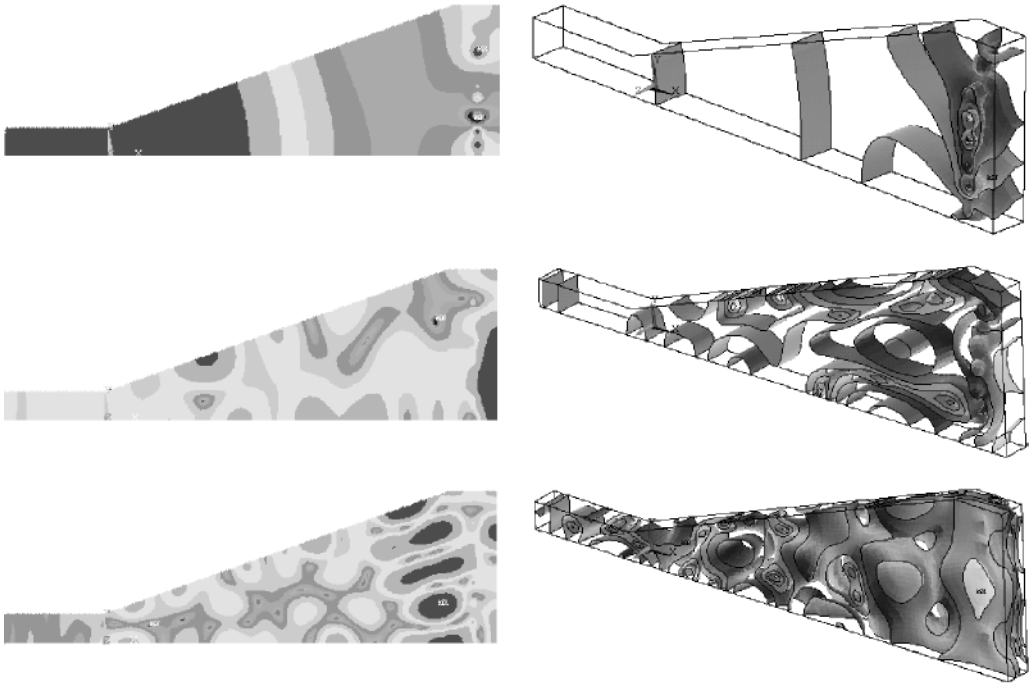
Figure 3. 2-D and 3-D iso-SPL surfaces at $f = 500$ Hz (top), $f = 2920$ Hz (mid) and $f = 5000$ Hz (bottom). Plane wave develops in the cross-squared section up to 3·4 kHz, above which the wave in no more plane.

thicknesses are fragile), the frequencies or the frequency range where the absorption coefficient $\alpha$ must be optimized (it is quite easy to obtain $\alpha = 1$ at a particular frequency but this reduces $\alpha$ at the other frequencies), the model of the porous materials to be used (several models with different complication and degrees of accuracy can be used) and, last but not least, the real availability of commercially available materials (which often need to be characterized experimentally to obtain the flow resistance $R(f)$, typically in the range 1000–80 000 rayls/m).

The overall length has been fixed at 300 mm with a maximum of three layers, each with a minimum thickness of 20 mm. The frequencies chosen for the optimization are the multiples of 100 Hz up to 800 Hz, above which $\alpha$ is almost unity for any possible stratification. The classical and relatively simple Delany and Bazley model for porous materials proved to be sufficiently correct in the flow resistance and density ranges of the materials used. As an analytical solution readily proved to be impossible as the inversion of a matrix (that is a product of several matrices) that contains hyperbolic functions is impossible, numerical simulations have been made by the use of the MATLAB Optimization Toolbox.

The optimization procedure consists of several steps:

1. an initial simulation has been made to estimate the best properties of the materials, by leaving the lengths of the layers $l_i$ *and* the flow resistances $R_i$ as converging parameters,

2. a selection of commercial materials test have been tested to cover the possible range of flow resistances $R$ required, after which the materials with $R$ closer to those given by step 1 have been chosen;
3. a second simulation has been made to determine the final configuration, fixing the flow resistances $R_i$ and leaving as converging parameters *only* the lengths of the layers $l_i$;
4. the final experimental verification of the properties of the termination.

The acoustical impedance $Z$ is defined as the ratio of the sound pressure and the velocity of the particle with $Z = p(x, t)/u(x, t)$. For air $Z_{air} = \rho c = 400$ rayls, where $\rho$ is the air density and $c$ is the sound speed in the air. The properties that define the behaviour of a sound absorbing material with respect to an incident plane wave are the normal incidence propagation constant $\gamma_0$ and the normal impedance $Z_0$ that are given, in the Delany and Bazley model [8], by

$$Z_0 = \rho c[1 + 0 \cdot 0571(\rho f/R)^{-0 \cdot 754}] - j\rho c[0 \cdot 0870(\rho f/R)^{-0 \cdot 732}], \qquad (2')$$

$$\gamma_0 = k[0 \cdot 189(\rho f/R)^{-0 \cdot 595}] + jk[1 + 0 \cdot 978(\rho f/R)^{-0 \cdot 700}], \qquad (2'')$$

where the flow resistance $R$ is defined as the pressure drop resulting in a 1 m/s airflow given by a 1 m thick specimen. The acoustical variables upstream and downstream of the arbitrary element $i$ along a pipe can be related with the transfer matrix (or four pole parameters) method that, for a multilayer termination, gives the global transfer matrix between upstream element 1 and downstream element $N$ (Figure 4) by partial matrices multiplication:

$$\begin{Bmatrix} p_i \\ u_i \end{Bmatrix} = \begin{bmatrix} T_{11} & T_{12} \\ T_{21} & T_{22} \end{bmatrix} \begin{Bmatrix} p_{i+1} \\ u_{i+1} \end{Bmatrix} = [T_i] \begin{Bmatrix} p_{i+1} \\ u_{i+1} \end{Bmatrix}$$

$$\Rightarrow \begin{Bmatrix} p_1 \\ u_1 \end{Bmatrix} = \prod_{i=1}^{N} [T]_i \begin{Bmatrix} p_{N+1} \\ u_{N+1} \end{Bmatrix} = [T] \begin{Bmatrix} p_{N+1} \\ u_{N+1} \end{Bmatrix}. \qquad (3)$$

For distributed porous elements the transfer matrix is given by

$$\begin{Bmatrix} p_i \\ u_i \end{Bmatrix} = \begin{bmatrix} \cosh(\gamma_i l_i) & Z_i \sinh(\gamma_i l_i) \\ \dfrac{1}{Z_i} \sinh(\gamma_i l_i) & \cosh(\gamma_i l_i) \end{bmatrix} \begin{Bmatrix} p_{i+1} \\ u_{i+1} \end{Bmatrix} = [T]_i \begin{Bmatrix} p_{i+1} \\ u_{i+1} \end{Bmatrix}, \qquad (4)$$
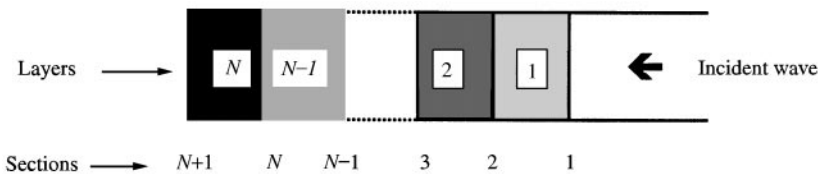


Figure 4. Layers and sections numbering for a multilayer anechoic termination.

For a rigid end $u_{N+1} = 0$, and then the inlet impedance is given by

$$\left\{\begin{matrix} p_i \\ u_i \end{matrix}\right\} = \begin{bmatrix} T_{11} & T_{12} \\ T_{21} & T_{22} \end{bmatrix} \left\{\begin{matrix} p_{N+1} \\ 0 \end{matrix}\right\} \Rightarrow Z_1 = \frac{p_1}{u_1} = \frac{T_{11}}{T_{21}}. \tag{5}$$

It should be noted that the reflection coefficient $r_1$ and the absorption coefficient $\alpha_1$ for the inlet section are given by

$$r_1 = \frac{Z_1 - \rho c}{Z_1 + \rho c}; \qquad \alpha_1 = 1 - |r_1|^2 \tag{6}$$

No details are given here about the experimental set-up and procedures necessary to test the various materials and the assembled termination, as they are made with a measurement chain that closely follows the norm ASTM 1050-86 [9] (Kundt pipe).

As a preliminary step it has been confirmed that the assumed model with the measured properties of some materials can correctly simulate the behaviour of a multilayered termination.

The goal function has been defined as $f(s_i, R_i) = \max(\Sigma\alpha(f))$, where $f$ is the vector of frequency previously mentioned. The materials have then been chosen and a further optimization has been made with the modified goal function $f(s_i) = \max(\Sigma\alpha(f))$, as the flow resistances $R_i$ were fixed. Numerical results are extremely good: $\alpha > 0.8$ at 125 Hz, while $\alpha > 0.95$ for $f > 210$ Hz. Experimental results completely confirm the simulation, and the results are compared in Figure 5.
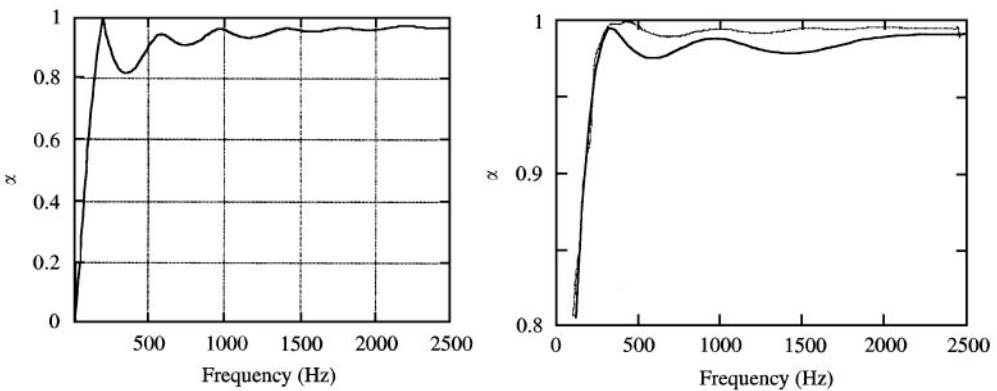


Figure 5. Absorption coefficient for three layers with $s_1 = 260$ mm, $R_1 = 1400$ rayls/m, $s_2 = 76$ mm, $R_2 = 3200$ rayls/m, $s_3 = 63$ mm, $R_3 = 6000$ rayls/m. Optimization at the frequency $f = 200$ Hz (left). Measured (- - - -) and simulated (——) $\alpha$ for the optimal solution with three layers with $s_1 = 140$ mm, $R_1 = 1500$ rayls/m, $s_2 = 100$ mm, $R_2 = 3500$ rayls/m, $s_3 = 60$ mm, $R_3 = 20\,000$ rayls/m. Optimization at the frequencies $f = 100, 200, 300, 400, 500, 600, 700, 800$ Hz (right).
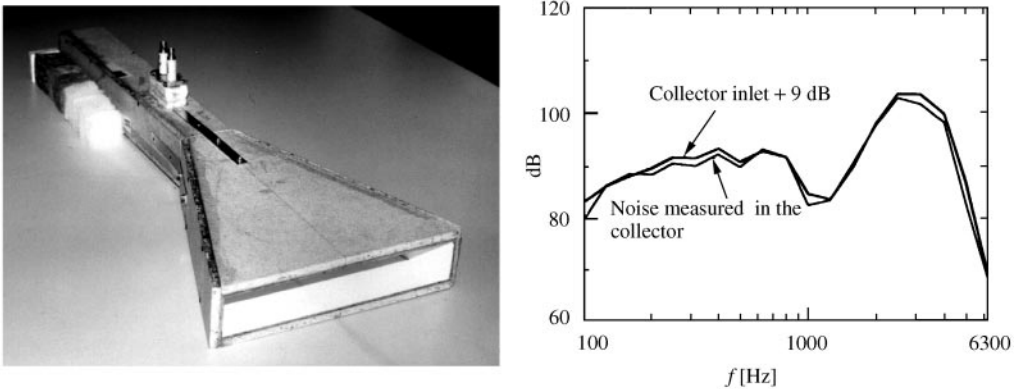
Figure 6. Prototype of the noise collector with materials used for anechoic termination (left). Comparison of inlet and measured inside the collector sound pressure levels. The SPL outside the collector has been increased by 9 dB to easy the comparison (right).

## 2.3. EXPERIMENTAL VALIDATION OF THE NOISE COLLECTOR

The prototype of the noise collector has been made of plywood covered with a hard layer to give a high reflection coefficient to internal walls (Figure 6). The validation of the device has been made through the measurement of the transfer function between two microphones, one inside the straight pipe and the other external to the collector in a position uninfluenced by the collector itself. The measurements have been taken in an acoustical free field with white noise up to 3·2 kHz generated by a laboratory reference sound source with broadband emission at a distance of 6 m from the device. The magnitude of the transfer function is particularly low ($< 5$ dB) confirming the FEM predictions. It must be noted that in a free field the SPL decreases by 6 dB by doubling the distance from the source or, equivalently, the sound pressure decreases by a factor $2^{1/2}$ doubling the area. In the noise collector the ratio between the inlet and outlet area is equal to 6, and so a 9 dB increase in the SPL is expected. The comparison of the $\frac{1}{3}$ octave band SPL measured by the microphones confirms this prediction (Figure 6); the lower frequency of practical use is 125 Hz, as below this frequency the termination absorption becomes insufficient and the limited measurement span (300 mm) is such that the very short acquisition time $T$ leads to very high statistical errors for limited bandwidths.

## 3. THE TRIPLE HORN FOR THE MEASUREMENT OF LATERAL UIC 60 RAIL EMISSION

The design of the device to be applied to the UIC 60 rail required some detailed design features. First of all the triple horn is subjected to a very high external noise coming from the passing wheel, and hence it must be made of sound insulating material. Moreover, it has to be attached to a structure that moves by several mm and that vibrates with very high levels, and the surfaces of the triple horn can themselves generate noise. Finally, cross-talk phenomena must be avoided as much
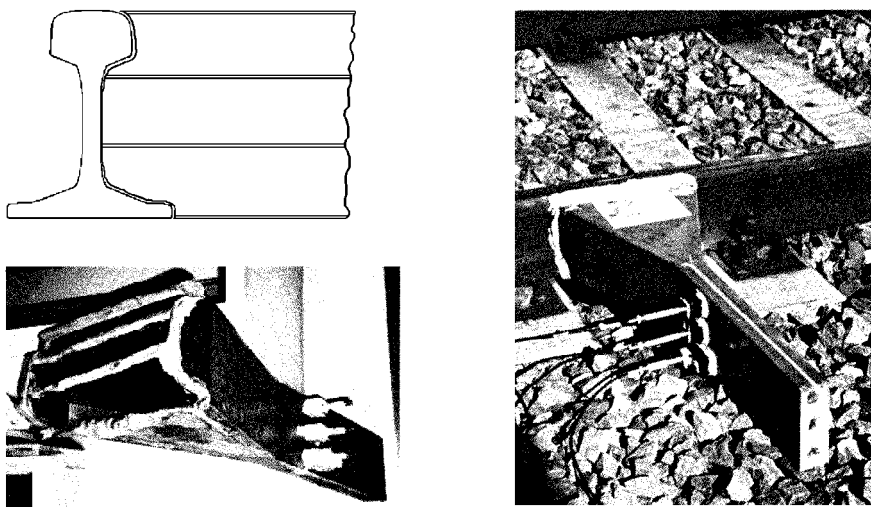
Figure 7. Sketch of the triple horn (top left), view in the lab (bottom left) and application along the railway line (right).

as possible, such that the noise measured by a microphone is not influenced by the noise present in the other ducts.

The cross-section of the final solution is shown in Figure 7. UIC 60 rail is 172 mm high; the three ducts are made with "silent steel", i.e., a sheet composed by two steel sheets with a viscoelastic material glued between them (constrained layer technique). This is sufficient to prevent high noise levels being generated by the vibrating surfaces of the triple horn, but to reach a sufficiently high level of sound insulation from external noise and to minimize cross-talk, two 3 mm silent steel sheets were used, reaching a total height of 174 mm. The inlet sections have been extended to match the UIC 60 rail profile as can be seen in Figure 7, where general views in the lab and during the measurement programme are also shown. The airgap between the inlet section and the rail has been sealed with putty, a classical solution in experimental acoustics that proved to be suitable here given the high quasi-static deformations of the rail. In the practice the solution demonstrated its validity, as putty remodelling was not necessary even after the passage of numerous trains.

## 4. MEASUREMENTS DESCRIPTION AND RESULTS

Tests on the noise emitted by the head, the web and the foot of an UIC 60 rail were performed in February 1998 during a noise and vibration measurement exercise on a test site on the railway line outside the Firenze Santa Maria Novella station towards Rome. Several types of passenger trains run on this line at speeds in the range 10–25 m/s. There were no macroscopic defects on the rail, but many train wheels were locally (wheelflat) or globally (polygonization) damaged.

The measurement chain included three measurement microphones flush-mounted on the straight pipes with their preamplifier and a digital computer
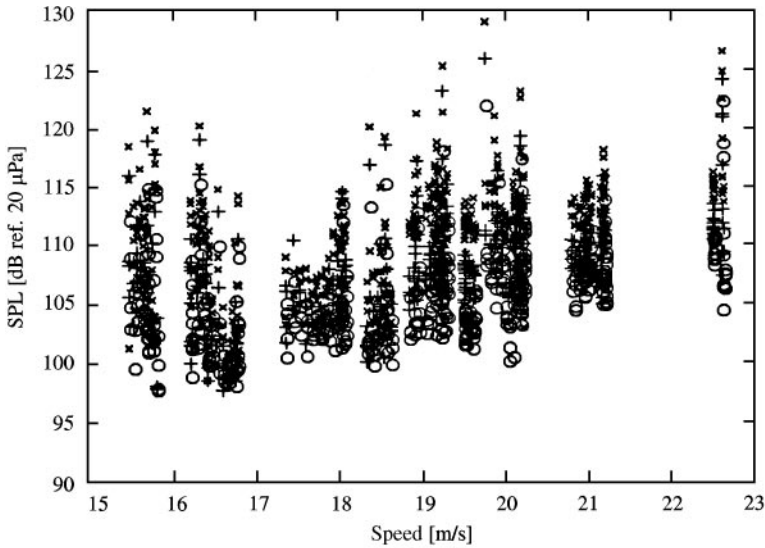
Figure 8. Corrected average SPL in the inlet section of the triple horn at the passing of all the analyzed wheels on the triple horn mounting section: + head, ○ web, × foot.

equipped with an acquisition card with anti-aliasing filters and a 16-bit ADC. Figure 8 shows the different SPL measured in the three ducts of the triple horn for several trains in this speed range. Each train is represented by a group of symbols at its passing speed. The SPL evaluation has been made by extracting from digital recording an equivalent length of 1·2 m (twice the distance between two sleepers) centred at the passing of each wheel and taking into account the different time duration for the different speeds. From this figure it can be seen that the noise increases with speed and that the different parts of the rail contribute in different manner to the global noise. In particular, as will be seen in the following, the web emits the least noise, while the contribution of the head is higher and the contribution of the foot still higher. The dispersion of the noise for some trains seems particularly high. Some drawbacks of the device are the intrinsic assumption of the stationarity of the sound field for a fixed distance (1·2 m) and the practical measurement only in the span between two sleepers. While the first assumption is necessary to make frequency content estimations stable, the second limitation does not appear to be significant. It is in fact practically impossible to distinguish, with energy-collector devices like this, the emission of slightly different portion of the rail; in the literature no study exists on the emission of the rail in the midspan or over the sleepers, but the feeling is that only a small change is likely to exist. The emission of the rail is considered symmetric with respect to the vertical plane of symmetry; no particular studies have been conducted on this subject, mainly because it is impossible to use the triple horn *inside* a track.

  Interesting experimental evidence can be extracted from the analysis of for instance, the noise measured by the upper horn, namely the one positioned on the head of the rail. Figure 9(a) shows the noise measured, corrected with the noise collector constant, for three different trains at the same speed. The fluctuation
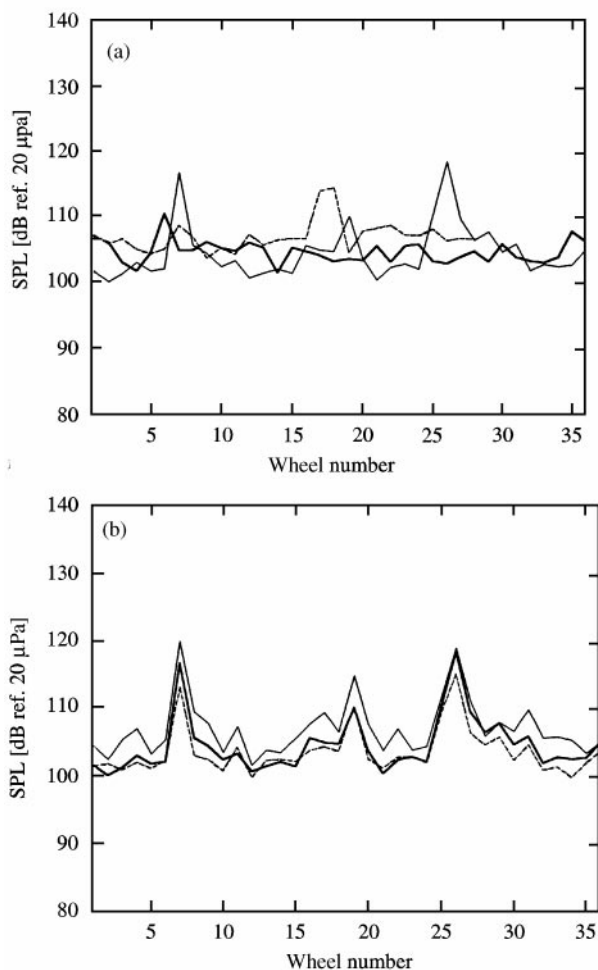
Figure 9. (a) SPL measured on the railhead for three trains running at around 18 m/s: thick line ETR 460, thin line 8MD (regional coaches) + D + E652 (loco not shown), dashed line E646 + 7PR (low floor) (loco not shown). (b) SPL measured for the train 8MD + B + E652 (loco not shown), 18 m/s (ca.): thick line: railhead, thin line: railfoot, dashed line: railweb.

around the average value is extremely limited for new rolling stock with disc-braked wheels with tread in very good condition, while for some trains in not such good condition the data scattering is significantly higher.

Further interesting information is obtained by comparing the results for noise levels emitted by the different portions of the rail at during the passage of a single train. Data for the typical regional train shown in Figure 9(a) are shown in Figure 9b, where it can be seen that the noise emitted by the head is always higher than the noise emitted by the web and lower than the noise emitted by the foot. Defective wheels are clearly recognizable and, especially for these, the contribution of the web can be high (wheel # 26), small (wheel # 19) or medium (wheel # 7). This behaviour is confirmed for all trains with defective wheels.
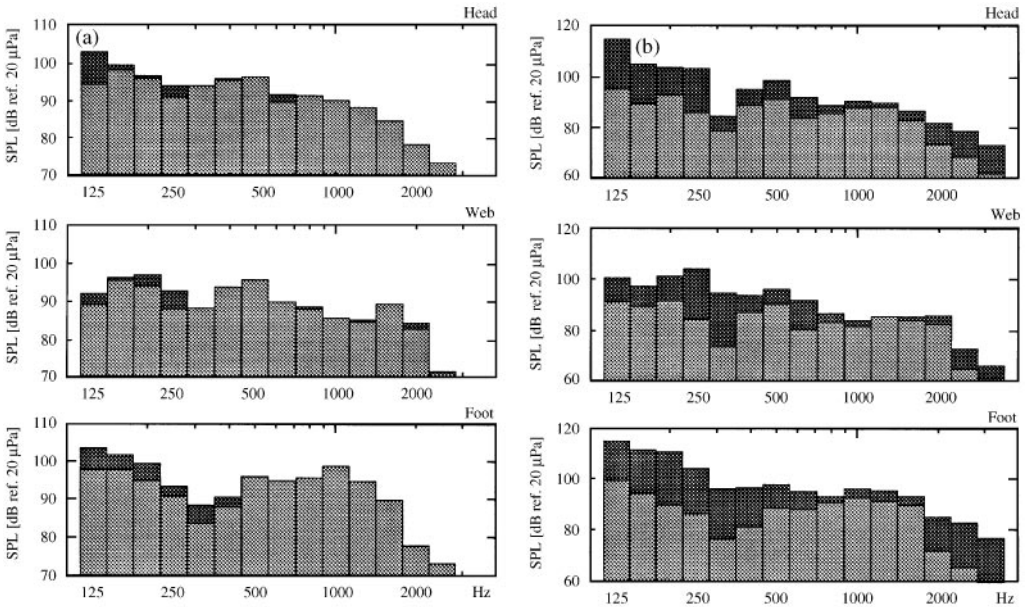
Figure 10. (a) Average $\frac{1}{3}$ octave band SPL for ETR460 (light) and 8MD + B + E652 (dark) trains. From top: head, web, foot. (b) $\frac{1}{3}$ octave band SPL for 8MD + B + E652 train. Wheel # 6 (not defective—light), wheel # 7 (defective—dark). From top: head, web, foot.

Constant percentage bandwidth frequency analysis for all the wheels of two trains running at the same speed are shown in Figure 10(a). The noise emitted by these trains is similar at higher frequencies, but the noise emitted by ETR460 is lower below 400 Hz, presumably because its wheels have a lower roughness.

The analysis of the noise emission during the passage of locally defective wheels (wheelflats) shows (Figure 10(b)) that not all the portions of the rail are equally sensitive to impacts given by this kind of defects. Moreover, some frequency bands are practically unaffected (see for example the 630–1600 Hz range) while others show increases up to 20 dB. Between these frequency bands particularly sensitive results are in the $\frac{1}{3}$ octave band centred at 250 Hz, where all the portions of the rail SPL increase by around 15 dB.

## 5. CONCLUSIONS AND FURTHER DEVELOPMENTS

The generic noise collector device briefly described in the first part of this work has been customized for the measurement of the noise emitted laterally by an UIC 60 rail. The initial results are extremely promising as they allow the direct and economic confirmation of present and future theories on the correct contribution of the rail noise to the global railway noise.

The simultaneous measurement of the ground noise with standard methodologies, the noise under the axlebox and the noise on the rail with the devices developed by the authors could be useful to identify correctly the various sources for many different vehicles at a limited cost.

## REFERENCES

1. A. BRACCIALI, L. CIUFFI, R. CIUFFI and P. RISSONE 1994 *Journal of Rail and Rapid Transit* **208**, 23–31. Continuous external train noise measurements through an on-board device.
2. A. BRACCIALI, L. CIUFFI and CIUFFI 1994 *Ingegneria Ferroviaria* **6**, 317–332. Metodo Innovativo per la Misura della Rumorosità Esterna dei Convogli Ferroviari.
3. A. BRACCIALI, L. CIUFFI and R. CIUFFI 1997 *Journal of Rail and Rapid Transit* **221**, 41–49. Calibration of an on-board noise measuring devices by simultaneous measurement of trackside noise of three different wheelsets for the ETR500 F. S. train.
4. L. E. KINSLER and A. R. FREY 1962 *Fundamentals of Acoustics.* New York: Wiley.
5. ANSYS 1995 *Acoustic and Fluid-Structure Interaction Manuals.* Houston, PA: Swanson Analysis System Inc.
6. A. BRACCIALI, and G. CASCINI 1997 *XXV Convegno AIA*, *Perugia*, *Italia*, 551–558. Un'attrezzatura per la misura del rumore emesso da una superficie vibrante.
7. A. BRACCIALI, and G. CASCINI 1997 *XXV Convegno AIA*, *Perugia*, *Italia*, 167–174. Ottimizzazione Acustica di una Terminazione Anecoica.
8. L. L. BERANEK 1971 *Noise and Vibration Control.* New York: McGraw-Hill.
9. ASTM E 1050-86 *American Society for Testing and Materials*, 1961 *Race St.*, *Philadelphia*, *PA* 19103. Standard test method for impedance and absorption of acoustical material using a tube, two microphones and a digital frequency analysis system.